ELSEVIER

Ceramics International 30 (2004) 2087–2098

CERAMICS INTERNATIONAL

www.elsevier.com/locate/ceramint

Synthesis of $La_{2-x}NiO_{4+\delta}$ oxides by polymeric route: non-stoichoimetry control

Marie-Laure Fontaine, Christel Laberty-Robert*, Antoine Barnabé, Florence Ansart, Philippe Tailhades

CIRIMAT/LCMIE, Université Paul Sabatier, UMR 5085, Bât II R1, 118 route de Narbonne, 31062 Toulouse Cedex 04, France

Received 3 October 2003; received in revised form 25 October 2003; accepted 19 November 2003
Available online 19 March 2004

Abstract

The synthesis of $La_{2-x}NiO_{4+\delta}$ oxides has been done via a polymeric route. This method allows the preparation of a wide range of non-stoichoimetry values. Oxides with values as high as 0.25 have been synthesised. Correlations between processing parameters such as sol composition and heat treatment have been done with structural and microstructural properties of the oxides. In our synthesis conditions, the higher the mean grain size, the higher the non-stoichoimetry level.

Transmission electron microscopy on these oxides has shown that whatever the non-stoichoimetry level, the extra-oxygen arranges in the structure according to two superstructures which correspond to $\delta = 0.25$ and $\delta = 0.17$. This shows that our grains consist of a mixture of these compositions.

Keywords: A. Sol–gel processes; B. Defects; B. Grain size; C. Ionic conductivity; E. Fuel cells

1. Introduction

Solid oxide fuel cells (SOFC) present much interests as a power generation system because of their high-energy conversion efficiency, fuel flexibility and environmental safety [1,2]. Typical SOFC with yttria-stabilised zirconia as electrolytes works at about 1000 °C. However, such high temperature operation causes degradation during a long-term service because of chemical interaction of cell components. One possible way to overcome this problem is to reduce the SOFC working temperature to 700–850 °C. Moreover, traditional cathode materials, i.e. $La_{1-x}Sr_xMnO_{3+\delta}$ (LSM), exhibit a relatively poor performance at this intermediate temperature, resulting from insufficient electrocatalytic activity and low ionic conductivity. A number of approaches have been taken in an effort to increase the electrochemical performance of the cathode materials by enlarging the electrochemical reaction zone. The use of mixed conducting electrode materials offers the advantage of an increase of the possible reactions pathways and provides a considerable decrease of polarisation losses. The mixed conductivity can be obtained by two approaches: mixing an ionically conducting material with an electronically conducting material to create a two-phase cathode (e.g. LSM/YSZ) or replacing the present materials with perovskites displaying high mix conductivity by changing the nature of transition metal on B-site by for example Co, Fe, and Ni, etc. [3,4].

In the perovskite structure, a good candidate is $La_{1-x}Sr_xCoO_{3-\delta}$ (LSC). Their ionic conductivity is among the highest for oxide ion conductor. In contrast to this ionic conductivity, the level of electronic conductivity is found to be relatively low, whereas the Mn analogue is found to have electronic conductivity of the order of 300 S cm^{-1}, but poor oxide ion conductivity. Moreover, the thermal expansion coefficients of the LSC materials are found to be high and cannot be used with the existing electrolytes. Studies have shown that the Co-doping on the B-site with Fe reduces the thermal expansion coefficient of the cathode material and consequently enables matching with the electrolytes [4].

As the development of the perovskite oxide compositions appears to be close to the optimum in term of mixed conduction, there has been increasing interest in alternative types of mixed conductors. Among the attractive alternatives to the

* Corresponding author. Tel.: +33-5-61-55-61-08; fax: +33-5-61-55-61-63.
E-mail address: laberty@chimie.ups-tlse.fr (C. Laberty-Robert).

0272-8842/$30.00
doi:10.1016/j.ceramint.2003.11.013

mixed conductors having perovskite or related perovskite structure is the K_2NiF_4 structure [5]. This structure consists of layers of ABO_3 separated by AO layers in which it is possible to incorporate excess oxygen in the unusual form of an interstitial species. This excess of oxygen provides an attractive alternative to the vacancy-based conduction mechanism present in the perovskite and fluorite oxides where the dopant−vacancy interaction can limit the observed conductivity. Compared to these latter oxides, this layered structure has a particular interest because it allows great flexibility in the oxygen stoichoimetry [9–14].

The aim of this study is to synthesise $La_{2-x}NiO_{4+\delta}$ ($0 \leq x \leq 0.04$) oxide via a polymeric route. We have adapted the approach of Gaudon and al. in which hexamethylenetetramine and acetylacetone in acetic acid with a ratio of 4.75 were used to prepare $La_{1-x}Sr_xMnO_{3+\delta}$ oxides [8]. We have extended this approach to synthesise $La_{2-x}NiO_{4+\delta}$ oxide with a wide range of non-stoichiometry levels by changing the processing parameters. In particular, the study of the nature of the sol, the complexing agent/transition metal (R = CA/TM) ratio, the heat treatment, the atmosphere during the sol decomposition has been made on the structure and microstructure of the oxides. In several recent reports, these oxides have been synthesised via solid–solid method.

Few studies report the synthesis of these materials via a soft chemistry process [15,16]. Powders of $La_2NiO_{4+\delta}$ oxides are synthesised at high temperatures (near 900 °C), using a modified sol–gel route. Despite of the high processing temperature, a value of $\delta = 0.18$ is reached for annealing in air and the structure of the $La_2NiO_{4.18}$ has been studied by neutron diffraction [15]. However, no report on the control of δ has been made.

In our studies, a wide range of non-stoichiometry oxides has been synthesised. Since modifying processing parameters such as heat treatment induces non-stoichiometry level changes, this approach offers an easy mean to control the non-stoichiometry level in this oxide and thus to prepare them with an adequate value of δ in term of the best mixed conductivity.

2. Experimental procedure

2.1. Sample preparation

$La_{2-x}NiO_{4+\delta}$ phases have been synthesised for various values of x and δ via a polymeric route. The polymeric precursors are prepared using solutions similar to the ones outlined by Pechini [6]. Solutions of metal nitrates, i.e. $La(NO_3)_3{\cdot}6H_2O$ and $Ni(NO_3)_2{\cdot}6H_2O$ are mixed in stoichiometric proportions and dissolve in deionised water. Since the cation concentration in the precursor is a critical parameter to obtain the pure La_2NiO_4 phase, a variety of molar concentrations is investigated [8]. Adding citric acid formed an organic–polymeric complex containing these metal ions. The citric acid to metal ions ratio is not constant and varies from 1 to 6. To this, ethylene glycol is added (citric acid to glycol ratio 1:1) to facilitate the formation of polymeric resin. During the heating, the poly-etherification reactions occur giving rise to the formation of a solid polymeric resin. This process is referenced P1. The polymeric structure breaks down above 400 °C and conduces to the char formation. The decomposed product is further heated at different temperatures from 600

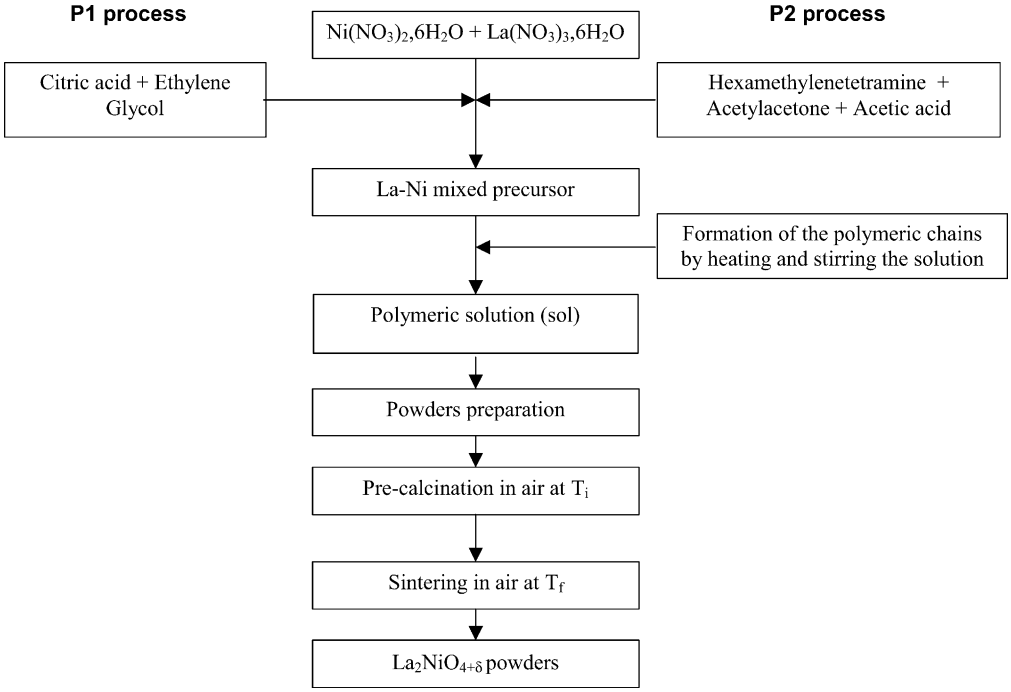

Fig. 1. Flow chart.

Table 1
Samples preparation

Notations	Type of resins	Concentration	r = La/Ni	R = CA/TM
P1(R; r)[a]	Ethylene glycol + citric acid	$0.1\,M \leq C \leq 0.6\,M$	$1.94 \leq r \leq 2$	$1 \leq R \leq 6$
P2(R; r)	HMTA + acetylacetone + acetic acid	$0.1\,M \leq C \leq 0.6\,M$	$1.94 \leq r \leq 2$	$1 \leq R \leq 3$

[a] Arbitrary notation used in this paper.

to 1000 °C in air for 2 h, to get crystalline phases of the oxides.

In order to study the effect of the nature of the resin on the oxides microstructure, the nature of the chelating and polymeric agents has been changed. This process is referenced as P2. It consists of the formation of a polymeric resin by condensation reaction between acetylacetone (Acac) and hexamethyltetraamine (HMTA) in acid acetic. The role of both HMTA and Acac is to complex the metal ions. The HMTA to metal ions is variable and varies between 1 and 6 while the HMTA/Acac ratio is constant and is 1:1. A flowchart for the preparation of these compounds is given in Fig. 1 and the different samples preparations are summarised in Table 1.

2.2. Thermal analysis

The non-stoichiometry δ of the oxides was determined through temperature programmed reduction followed by thermogravimetric analysis. The experiment was carried out in a vertical lug flow reactor. The mass variation of the oxide (initially 80 mg) was followed with a Cahn D200 electrobalance. The sample was first depressed (1 Pa) at room temperature for 1 h and the reactor was filled with a mixture of 10%H_2/Ar, maintaining a flow of 15 $cm^3\,min^{-1}$. The temperature was then linearly increased with a heating rate of 5 $K\,min^{-1}$ up to 900 °C. The technique presents the advantage to quantify selectively the non-stoichiometry oxygen, without preliminary dissolution as in chemical titration methods. Of course, this method can only be used if the heating of the non-stoichoimetric oxides gives single stoichoimetric oxide such as La_2O_3 and metal like Ni.

Thermogravimetric (TGA) and differential thermal analyses (DTA) were carried out on a Setaram TG-DTA 92 microbalance with 20 mg of sample and alumina as a reference. The experiments were performed in air at a heating rate of 5 $K\,min^{-1}$ from room temperature to 1000 °C.

2.3. X-ray diffraction analysis

The determination of the crystallographic structure of the powders sample was performed by X-ray diffraction with a Seifert XRD 3003 TT diffractometer using the Cu Kα radiation (λCu Kα1 = 1.5405 Å and λCu Kα2 = 1.5443 Å). All data were synthesised using profile matching analysis and Rietveld method implanted in the Fullprof program [20,21] for crystal structure refinement.

2.4. Chemical analysis

The chemical compositions were determined by atomic absorption spectroscopy. The La/Ni ratio is found to be slightly higher than two for $r = 2$.

To confirm the non-stoichiometry levels evaluated from TG analyses, titrations are done according to chemical method [7]. The non-stoichiometry level is directly correlated to the content of Ni^{3+} to respect the electroneutrality of the compound. Thus, the determination of Ni^{3+} level via an iodometric titration allows the evaluation of δ.

2.5. Electron microscopy

Scanning electron microscopy (SEM) (JEOL-JSM-35CF) was used to observe the morphology and the microstructure resulting from the various sintering conditions.

Transmission electron microscopy (TEM) observations were performed with a JEOL 200 CX electron microscope operating at 200 kV and equipped with a tilt-rotation sample holder. Experiments were performed at room temperature. Specimens were prepared by grinding and crystallites were deposited on a holey carbon film. The electron diffraction (ED) patterns were obtained by selected area diffraction.

3. Results and discussion

3.1. Precursor characterisation

In order to determine the best annealing treatment, a thermal analysis was performed under air. Fig. 2 shows the TG and DT curves of the La_2NiO_4 polyester resin treated at 200 °C during a night in air for both processes. Fig. 3 shows the ratios m/e = 14, 44, 30 due to CO, CO_2, NO and NO_2 for both processes P1 and P2, respectively. For this study, both ratios of chelating agent to transition metal oxide (R) and Lanthanum to Nickel metal oxide (r) are constant and remained at 2.

The thermal analyses of both processes turn out to be complex. For the P1 process, thermal analysis reveals a three-step weight loss with corresponding DTA curves. The first weight-loss, which occurs at around 90 °C, corresponds to the elimination of water compounds that were not removed during the initial solution drying process. The second major weight loss occurs between 300 and 600 °C, and it is

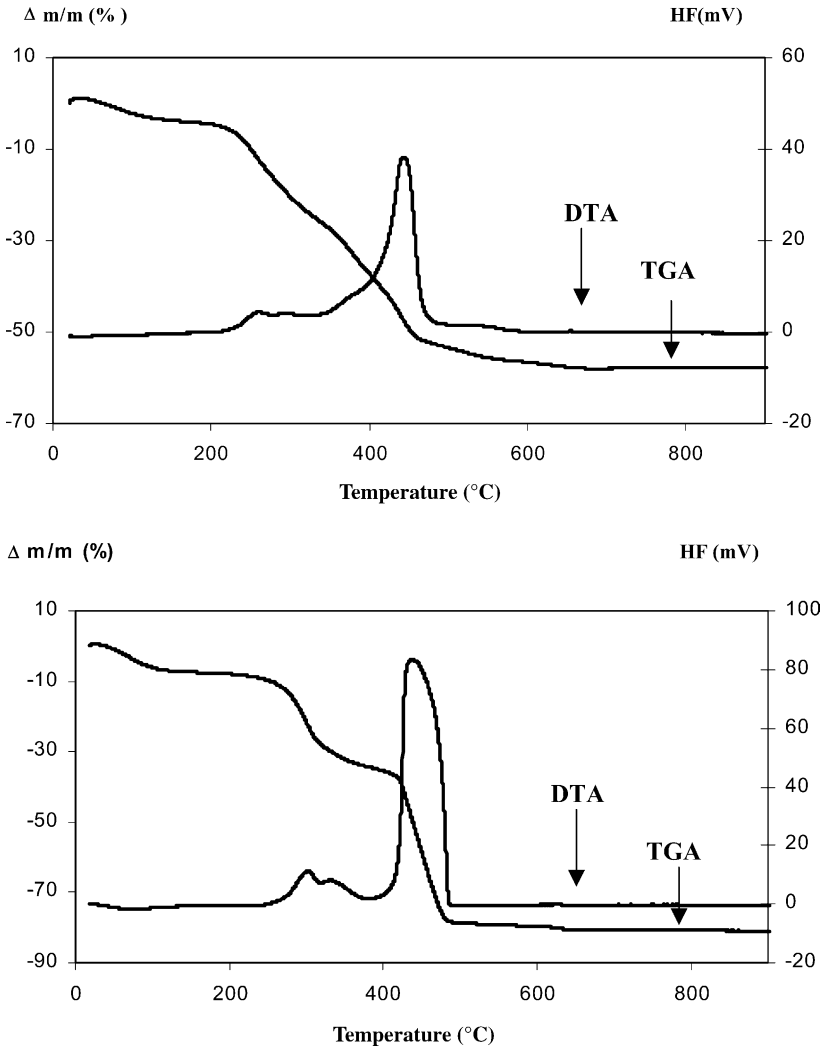

Fig. 2. DTA and TGA curves of the precursor prepared from P1 (a) and P2 (b) processes.

caused by the burnout of pyrolised organics. The *m*/*e* curves show that this step corresponds to the decomposition of organics and nitrate species. As it can be seen, it is difficult to separate each species.

The third weight loss around 700 °C may be attributed to the decomposition of an amorphous oxycarbonate formed during the previous step [8]. This is confirmed by the ratio *m*/*e*. It appears a small peak at 700 °C of the ratio $m/e = 44$. There is no more weight loss above 700 °C. These results are confirmed by DTA experiments. Indeed, the DTA results show an endothermic reaction starting at 90 °C related to water loss and exothermic reactions starting at 300 °C related to the decomposition of the organics and nitrates species and La_2NiO_4 formation.

Thermal analysis of the P2 process is similar to the one observed for P1 process and reveals also a three-step weight loss. Moreover, in this case the sol decomposition appears to be faster.

To evaluate the influence of temperature on the formation of the oxide, the polyester resin was directly heated to 400 °C with a heating rate of 2 °C min^{-1} for the decomposition of the organic material and then calcinated at various temperatures for 2 h. A low heating rate has been used in order to avoid that the reactions occurring during the heating carry away.

3.2. Effect of the sol composition on the structure and microstructure of the oxides

3.2.1. Effect of the ionic concentration on the phase purity

To evaluate the influence of the ionic concentration on the structure of the oxides, several polymeric resins have been synthesised with various ionic concentrations ranging from 0.075 to 0.60 mol l^{-1}. Both *R* and *r* ratios were fixed at 2. For both processes, the concentrations below to 0.15 mol l^{-1} lead to the formation of the pure phase. Intergrowth of $La_3Ni_2O_7$ phases and La_2O_3 oxides are observed above this value. Thus, the concentration of 0.15 mol l^{-1} is defined as the limit concentration for the synthesis of pure $La_2NiO_{4+\delta}$ powders.

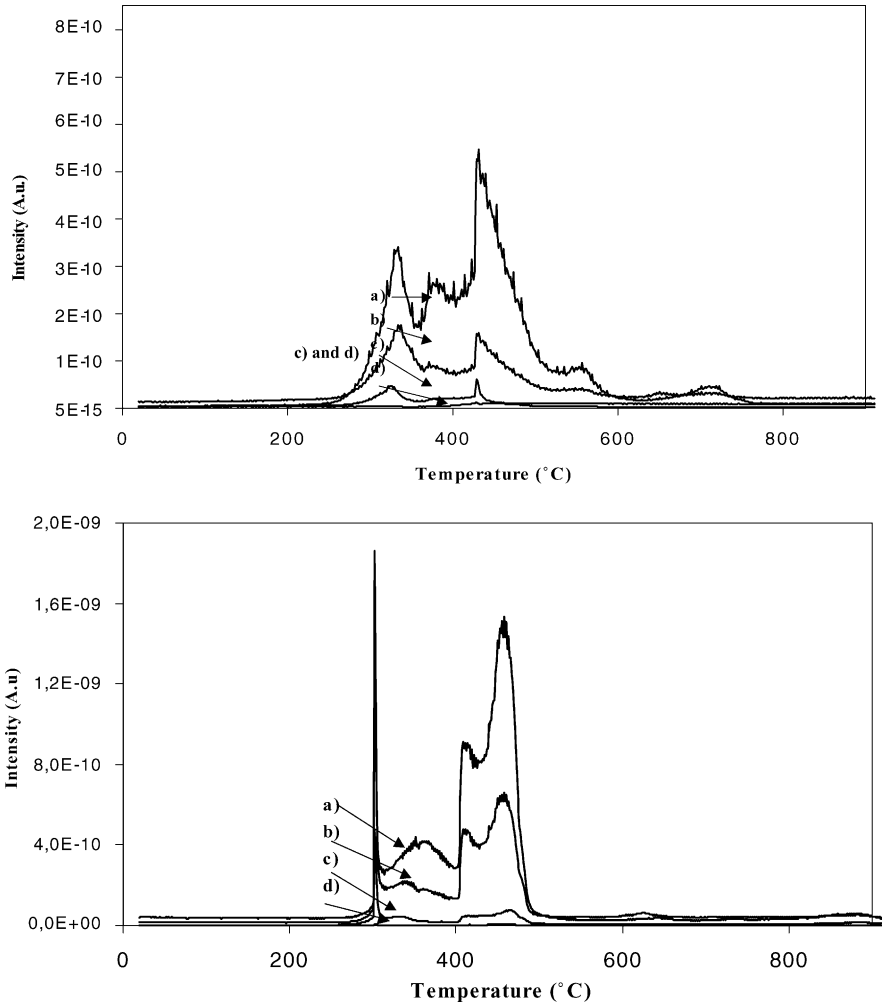

Fig. 3. Mass spectrometry of the precursor from P1 (1) and P2 (2) processes: (a) $m/e = 44$, CO_2, (b) $m/e = 28$, CO, (c) $m/e = 30$, NO, (d) $m/e = 46$, NO_2.

3.2.2. Effect of the processing parameters for the sol preparation on the microstructure of the powders

The non-stoichoimetry levels and the structure of $La_2NiO_{4+\delta}$ oxides have been studied as a function of the *R* ratio for both processes P1 and P2. This ratio varies from 1 to 6 for P1 process, while for P2 it is in-between 1 and 3. This is due to the stability of the polymeric resin. In the P2 process, when the *R* ratio increases, the pH increases and reaches value above 3. In this range, there is precipitation of nickel hydroxide.

XRD patterns of $La_2NiO_{4+\delta}$ powders calcined at 1000 °C in air for 2 h are shown in Fig. 4 for both processes. It can be obviously seen from the XRD that the pure $La_2NiO_{4+\delta}$ phase is obtained for $2 \leq R < 4$ while for $R < 2$, intergrowth of $La_3Ni_2O_7$ phases and La_2O_3 oxides form. These results show that the complexation of the metallic cations is not homogeneous for low organic content. To ensure a complete and homogeneous cations chelation, the *R* limit ratio is about 2.

For P1 process when $R \geq 4$, the samples are a mixture of $La_{2-x}NiO_{4+\delta}$ and La_2O_3 oxides. For this range of *R*, the complexation of cations inside the polymeric solution is homogeneous. However, beside the Ruddlesden Popper oxide, La_2O_3 oxides are obtained. An explanation is the heat release during the decomposition of the sol, which is more important when *R* increases. This may destroy the cation homogeneity and then induces the formation of La_2O_3 oxide. To verify this hypothesis, differential thermal analyses have been performed in air for gel with different *R* ratios. The higher the *R* ratio, the higher the exothermicity of the reaction [9]. The heat released during the decomposition process is due to oxido-reduction reactions, which occur between organic and nitrate species. From these results, it appears that when the organic/nitrate ratio increases the reaction is more exothermic.

Sols with $R = 4$ and La/Ni ratio below to 2 have then been synthesised with the aim of confirming these. Indeed, this induces the decrease of the amount of NO and NO_2 gazes generated during the decomposition. These experiments have been carried out with only the P1 process because in the P2 one, it is difficult to control the amount of nitrate due to the presence in the HMTA compound

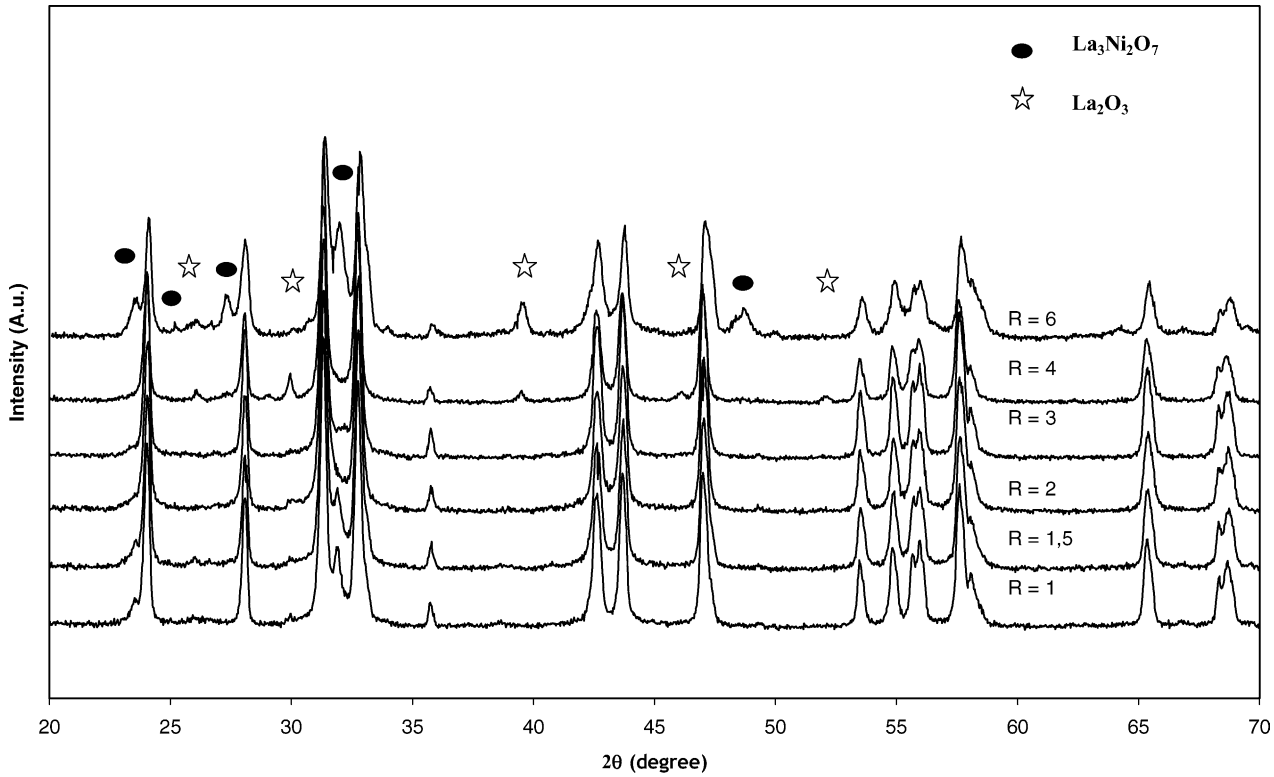

Fig. 4. X-ray diffraction patterns of powders prepared from different R ratio for both processes with $r = 2$.

of nitrogen. Table 2 summarises results. As it is seen for $R = 4$, the $La_{2-x}NiO_{4+\delta}$ phase forms for $2 < x < 1.94$. When $R > 4$, the decrease of the La/Ni ratio does not allow us to obtain pure phases. This means that the nitrate content in solution is still enough to have strong exothermic reactions which could not be controlled even if a very low heating rate is used during the sol decomposition.

Experiments have been performed for $R = 1$ and no pure phase is obtained. It seems that for low R-values, the decrease of the La/Ni ratio cannot supply the inhomogeneity in the sol at the cationic levels.

From these results, it appears that the R and r ratios are key parameters to obtain the pure Ruddlesden Popper phases. The homogeneity in the sol has to be first reached and then the exothermicity of the reaction has to be controlled.

The non-stoichoimetry level of $La_{2-x}NiO_{4+\delta}$ phases has been established for $2 \leq R \leq 4$ and $2 \leq r \leq 1.96$. Table 3 reports both δ and Ni^{3+} values (τ).

For $r = 2$, the non-stoichoimetry is a function of both the R ratio and the nature of the chelating and complexing agents. Higher values are obtained for P2 process than the P1 one. This is linked to the oxidising atmosphere developed during the decomposition of the sol. Assuming that the oxidising conditions are correlated to the presence of nitrogen oxides, in P2 process these conditions come from the decomposition of both the nitrates and the hexamethylenetetramine, which also produces nitrogen oxides during its heating decomposition. This explains the higher values of δ for oxides prepared from P2 process and the increase of the Ni^{3+} (τ) while increasing the R ratio.

However, this difference is not yet observed when the r ratio decreases. The value of the non-stoichoimetry is the same for a given r and R. According to Greenblatt [10], the non-stoichiometry is due to the excess of oxygen and to charge compensating Ni^{3+} ions (hole). These stabilise the K_2NiF_4 structure by both reducing the intrinsic charge

Table 2
Influence of the r ratio and the organic content on the formation of La_2NiO_4 powders for both processes P1 and P2, $T = 1000\,^{\circ}C$, 2 h, in air

For P1 and P2 processes				For P1 process	
r = La/Ni	$R = 1$	$R = 2$	$R = 3$	$R = 4$	$R = 6$
2	Mixture b^o	$La_2NiO_{4+\delta}$	$La_2NiO_{4+\delta}$	Mixture b^o	Mixture a*
1.98	Mixture a*	$La_{2-x}NiO_{4+\delta}$	$La_{2-x}NiO_{4+\delta}$	$La_{2-x}NiO_{4+\delta}$	Mixture a*
1.96	Mixture a*	$La_{2-x}NiO_{4+\delta}$	$La_{2-x}NiO_{4+\delta}$	$La_{2-x}NiO_{4+\delta}$	Mixture a*
1.94	Mixture a*	Mixture a*	Mixture a*	Mixture a*	Mixture a*

Mixture a*: $La_2NiO_{4+\delta} + La_2O_3 + La_3Ni_2O_7$; mixture b^o: $La_{2-x}NiO_{4+\delta} + La_2O_3$.

Table 3
Evolution of δ as a function of La/Ni and CA/TM ratio for powders prepared from P1 and P2 process, calcined at 900 °C in air for 2 h

R = CA/TM	r = La/Ni	τ Ni^{3+} (±0.01)	δ (±0.01)
P1 process			
$R = 2$	2	0.34	0.17
	1.98	0.33	0.14
	1.96	0.37	0.13
$R = 3$	2	0.36	0.18
	1.98	0.30	0.12
	1.96	0.35	0.12
$R = 4$	1.98	0.29	0.12
	1.96	0.30	0.09
P2 process			
$R = 2$	2	0.38	0.19
	1.98	0.32	0.13
	1.96	0.38	0.12
$R = 3$	2	0.44	0.22
	1.98	0.30	0.12
	196	0.35	0.12

separation between the electropositive La_2O_2 and NiO_2 layers and the structural strain due to the misfit between these two layers [10]. These cations oxidations allow to preserve the overall electrical neutrality of the crystals.

Therefore, the formation of $La_{2-x}NiO_{4+\delta}$ oxide with lanthanum vacancies induces an increase of the Ni^{3+} (τ) content compared to the stoichiometric one. This will induce modification on the non-stoichiometry level (δ). From our studies, it can be seen that the δ value decreases when the r ratio decreases. The decrease of δ is mostly due to the decrease of extra oxygen in the structure. Indeed, the Ni^{3+} content does not vary that much when r decreases. As an example, the decrease of r from 2 to 1.96 would involve the oxidation of 0.04 Ni^{2+} to Ni^{3+}. If we compare the Ni^{3+} content for $r = 2$ and $r = 1.96$, it can be seen that this variation is not observed, the Ni^{3+} value remains constant or decreases.

3.3. Effect of the heat profile on the structure and microstructure of the oxides: intermediate temperature, annealed temperature, and atmosphere

As previously shown, controlling the sol parameters R and r can modulate the non-stoichiometry level of the $La_{2-x}NiO_{4+\delta}$ ($x \geq 0$) oxides. Another way to optimise the non-stoichiometry level is to control the temperature profile and the atmosphere during the sol decomposition. Thermal analyses for P1 and P2 processes have shown that the most weight loss occurred below 400 °C and the decomposition ends up at 600 °C. Accordingly, two intermediate temperatures have been chosen: 400 and 600 °C. The low heating rate of 2 °C min^{-1} has been used in order to control the exothermicity of the reactions and then to avoid that the decomposition of the reaction carries away.

Table 4 summarises the X-ray results of $La_2NiO_{4+\delta}$ for both intermediate temperatures. Samples with $T_i = 400$ °C are single phase having an orthorhombic crystal structure (*Fmmm* space group) while samples with $T_i = 600$ °C show impurity. This is probably due to the difficulty to control the decomposition of the gel when the intermediate temperature is after the end of decomposition of the dried gel. Therefore, it is necessary to control the intermediate temperature during the heat treatment of the dried gel. The acceptable intermediate heat treatment should be around 400 °C.

Table 4
Influence of the intermediate temperature T_i for P1 and P2 processes with r = La/Ni = 2

Type of synthesis	R	$T_i = 400$ °C	$T_i = 600$ °C
P1 process	2	$La_2NiO_{4+\delta}$	$La_{2-x}NiO_{4+\delta} + La_2O_3$
	3	$La_2NiO_{4+\delta}$	$La_{2-x}NiO_{4+\delta} + La_2O_3$
P2 process	2	$La_2NiO_{4+\delta}$	$La_2NiO_{4+\delta}$
	3	$La_2NiO_{4+\delta}$	$La_{2-x}NiO_{4+\delta} + La_2O_3$

The non-stoichiometry level for pure $La_2NiO_{4+\delta}$ oxides shows that δ decreases when increasing T_i. As an example, for P1(2,2) sample annealed at 900 °C, $\delta = 0.15$ for $T_i = 600$ °C while $\delta = 0.16$ for $T_i = 400$ °C.

These results show that the intermediate heat treatment influences the nature and the properties of the oxide.

After the intermediate heat treatment, the powders are grinded and then annealed in air for 2 h at temperatures ranging from 600 to 1000 °C with a heating rate of 100 °C/h. Fig. 5a and b show the X-ray powder diffraction patterns of $La_2NiO_{4+\delta}$ for P1(2;2) and P2(2;2) samples. Whatever the synthesis, the same behaviour is observed. Diffuse XRD patterns are obtained for powders heat treated at 600 and 400 °C, indicating that the precursors are amorphous. For temperatures above 700 °C, the $La_2NiO_{4+\delta}$ phase forms. Thus, $La_2NiO_{4+\delta}$ oxide is likely to nucleate from an inorganic amorphous matrix and forms in between 700 and 800 °C.

From these studies, it has been shown that the oxides annealed above 700 °C, crystallise in the orthorhombic symmetry with the *Fmmm* space group within the conditions for this study. A comparison of the X-ray diffraction patterns of P1(2;2) and P2(2;2) samples shows that an increase of the orthorhombicity (the *a*/*b* ratio increases) is observed for P2(2;2) sample. According to Tamura et al. [13], this is a characteristic behaviour of the *Fmmm* phase in $La_2MO_{4+\delta}$ system (M = Ni, Cu). They found that this symmetry is obtained for $La_2NiO_{4+\delta}$ oxides with a δ above 0.15. This result shows that our oxides present non-stoichiometry level higher than 0.15. Indeed, the non-stoichiometry levels evaluated for P1(2;2) and P2(2;2) samples are 0.16 and 0.18, respectively.

For $La_{2-x}NiO_4$ sample with $x > 0$, the oxides adopt the K_2NiF_4 structure, which crystallises in the space group *I4/mmm*.

From the data refinements, the lattice parameters and the crystallites size of the oxides have been determined. The results showed an evolution of the lattice parameters

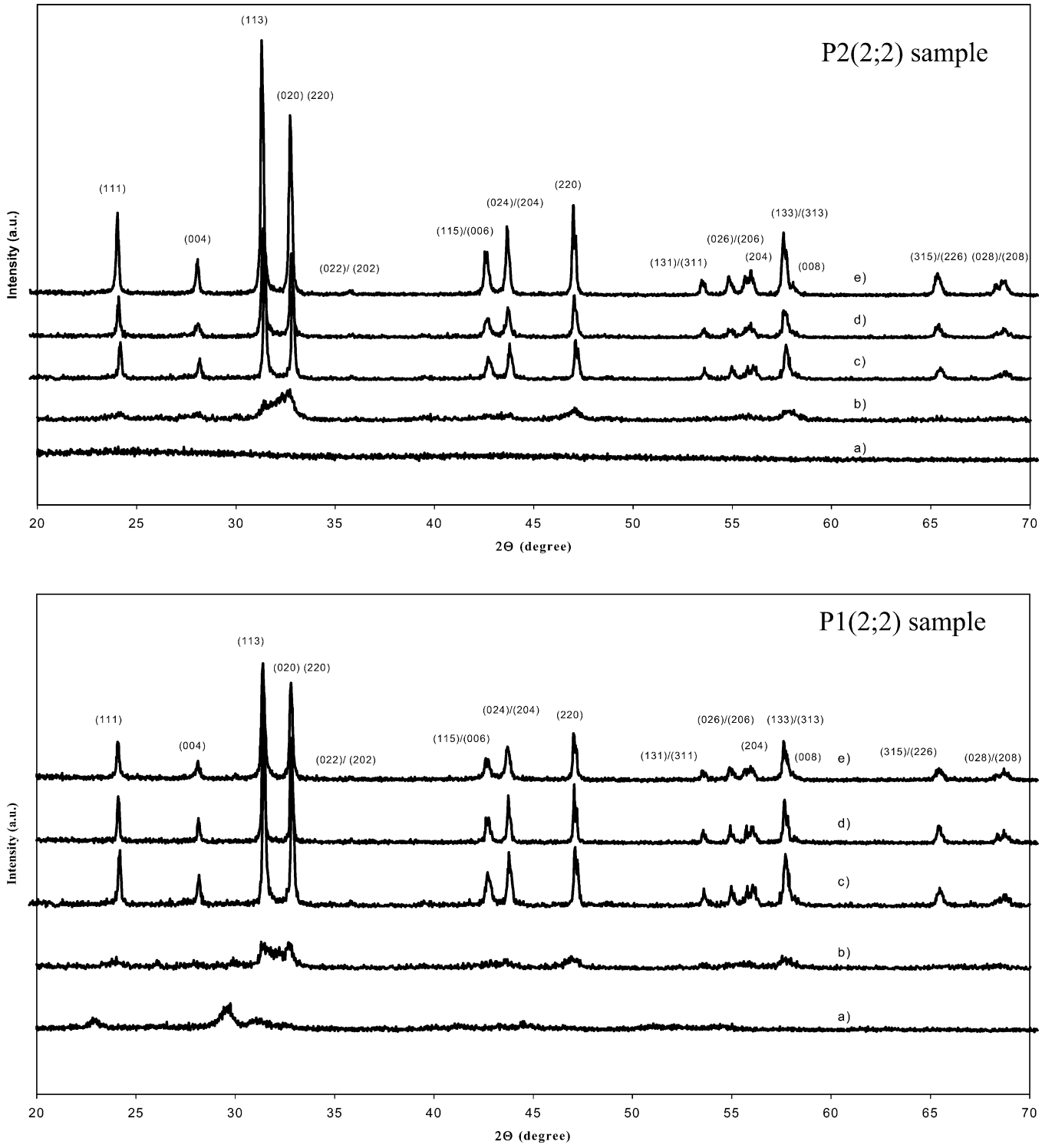

Fig. 5. XRD of $La_2NiO_{4+\delta}$ powders calcinated in air for 2 h at different temperatures. (a) 600 °C, (b) 700 °C, (c) 800 °C, (d) 900 °C, (e) 1000 °C.

depending on the non-stoichiometry level. This evolution was also correlated to the average size of the grains ($\langle d \rangle$). In Table 5 are reported the values of $\langle d \rangle$ evaluated from scanning electron microscopy and the lattice parameters determined by the X-ray data refinement. Values of δ are also reported in Table 5.

Fig. 6 presents the evolution of $\langle d \rangle$ as a function of δ. The results expected are an increase of δ while $\langle d \rangle$ decreases. This is a common behaviour of the evolution of the non-stoichiometry level as a function of the mean grain size for perovskite oxide [8]. On the contrary in our studies, the average of the mean grains size increases with

Table 5
Evolution of the lattice parameters and the mean grain size as a function of δ

References	Heating temperature (°C), 2 h	δ TGA (±0.01)	δ Chemical titrations (±0.01)	$\langle d \rangle$ (±10 nm)	Lattice parameters	Lattice volume (Å^3)
P2(2;2)	900	0.19	0.19	120	$a = 5.453(5)$ Å $b = 5.462(9)$ Å $c = 12.697(8)$Å	377
	1000	0.18	0.18	160	$a = 5.458(6)$ Å $b = 5.463(2)$ Å $c = 12.686(1)$ Å	378
P1(2;2)	900	0.17	0.16	80	$a = 5.460(1)$ Å $b = 5.458(9)$Å $c = 12.683(7)$ Å	378
	1000	0.16	0.16	100	$a = 5.465(4)$ Å $b = 5.459(5)$Å $c = 12.684(5)$ Å	378

increasing δ and this evolution seems to be relatively linear for a given annealing temperature. An increase of $\langle d \rangle$ from approximately 50 nm is attended with an increase of δ from about 0.01. This behaviour is available in our experimental process conditions and is correlated to the sols decomposition. The stabilisation of the Ni^{3+} content depends on the nature of the atmosphere during the decomposition of the dried gel. As shown previously, this stabilisation is more important for powders issued from P2 process.

The difference of both the heat released during the decomposition and the nature of the atmosphere between the two processes conduces to higher particles size for powders issued from P2 process. As an example, for P1(2;2) and P2(2;2) samples annealed at 1000 °C, δ is 0.16 and 0.18, respectively, while $\langle d \rangle$ is 100 and 160 nm, respectively. The more the oxidant atmosphere, the more the exothermic reactions, the higher values for δ and $\langle d \rangle$.

Fig. 7 shows the evolution of the lattice parameters as a function δ for oxides synthesized with variable R ratio in order to have a wide range of δ.

For δ increasing from 0.16 to 0.19, it can be observed a slight decrease of the a-parameter from 5.465 to 5.453 Å while the c-parameter remained almost constant, ranging from 12.683 to 12.697 Å. These results are explained by the literature. As there is a misfit between the both layers La_2O_2 and NiO_2, a stress in the (a,b) plane appears, leading to a tilt of the MO_6 octahedra along the $[0\,1\,0]_{Bmab}$ direction. The relief of this equatorial compressive stress can be achieved by both oxidising the M^{2+} cation (electronic effect) and introducing additional oxygen atoms (steric effect) [15,25]. These both effects appear simultaneously, but depending on the composition of δ, one effect can be predominant. For compositions ranging from 0.12 to 0.17, both electronic and steric effects are responsible for the typical evolution of the lattice parameters (decrease of the a and b parameters while c increases) often sees in the literature [12–14]. For composition above 0.17, the absence of change in the c parameter results from the fact that the steric effect is compensated by the electronic effect in the NiO_2 layer [15,22].

Accordingly, our results show that for high compositions of δ, no change of the lattice parameters is observed and thus, the relief of the internal stresses for our oxides results from a strong electronic effect.

The lattice volume of our oxides has been calculated. No significant change in the lattice volume as a function of δ

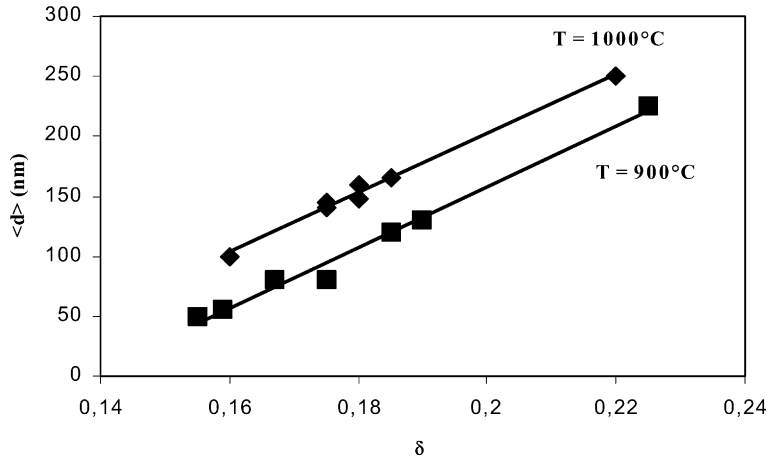

Fig. 6. Evolution of $\langle d \rangle$ as a function of heating temperature and non-stoichiometry level.

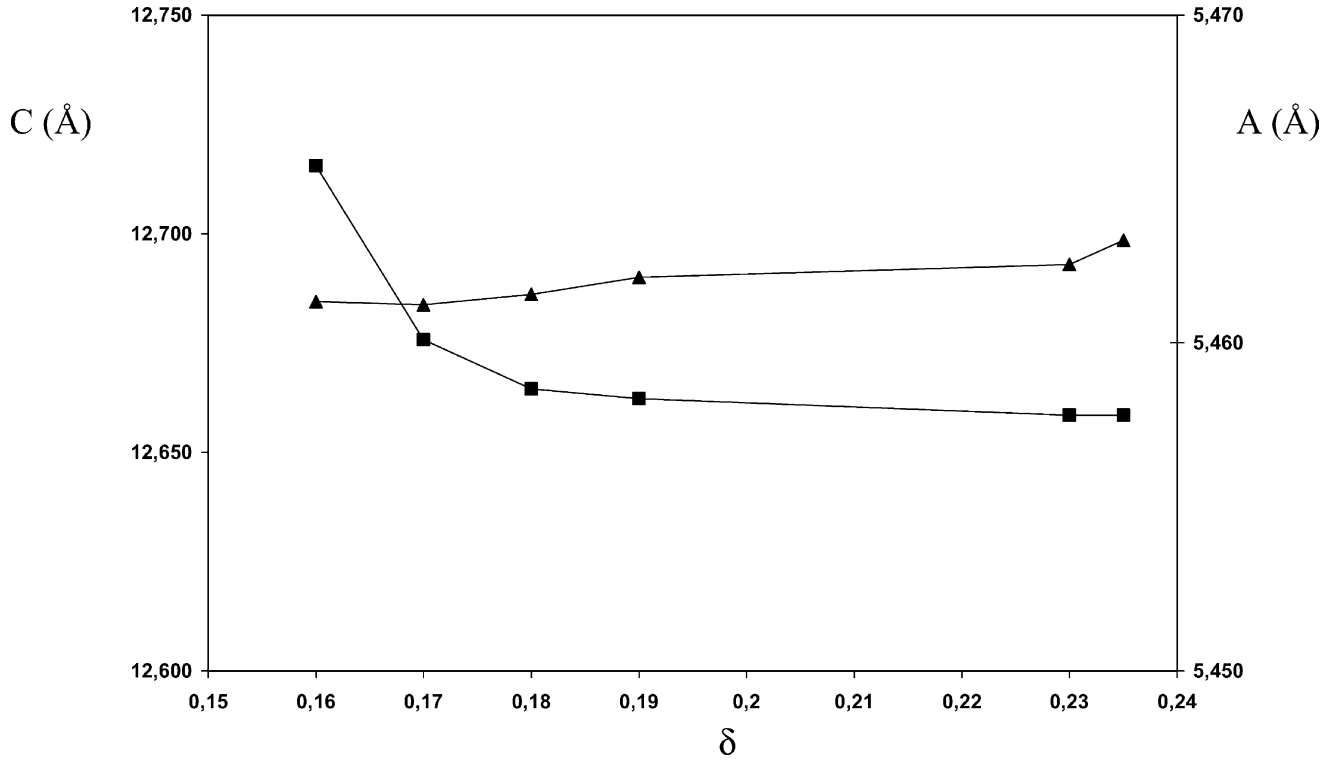

Fig. 7. Evolution of the lattice parameters $C(\tilde{A})$ and $A(\tilde{A})$ as a function of δ in $La_2NiO_{4+\delta}$ with variable R ratio.

is observed, as shown in Table 5. This is in agreement with our previous result.

In order to explain the evolution of the lattice parameters when δ is modified, and better understand the intercalation reaction mechanism of oxygen, transmission electron microscopy observations have been made.

Two different samples $La_2NiO_{4.19}$ and $La_2NiO_{4.25}$ have been studied. Some ED patterns are presented in Fig. 8a–c.

The reconstitution of the reciprocical lattice from different electron diffraction patterns shows that the crystal symmetry of the host structure for both samples is orthorhombic *Fmmm* with the following lattice parameters: $a \approx 5.50$ Å, $b \approx 5.50$ Å, $c \approx 12.70$ Å. This is in agreement with the XRD results. The main spots on the micrographs identify the host structure. Depending on the observed crystal, a wide variety of superlattice reflections have been observed in ED patterns; all of them exhibit small spots in addition to the main spots. Their presence is attributed to the ordering of excess oxygen atoms. These superlattice spots are aligned along the $[1\,1\,1]^*$ direction and depending on the ED patterns, one can observe that the $[1\,1\,1]^*$ direction is divided in $n = 2$ or $n = 3$ intervals. The $n = 2$ and $n = 3$ patterns for $La_2NiO_{4.25}$ oxide are shown on Fig. 8a and b. Hiroï and al. describe this superstructure as $2a \times ka \times lc$ (k, $l = n$ or $2n$ depending upon n) where $a \times a \times c$ stands for the K_2NiF_4-type cell [18]. This model gives excess oxygen contents of $1/2n$ for arbitrary n [23–25]. As shown on the ED patterns of Fig. 8, both $n = 2$ and $n = 3$ patterns are obtained for $La_2NiO_{4.19}$ and $La_2NiO_{4.25}$ oxides. This reveals the existence of domains in which the composition of δ is either 0.17 or 0.25 for both samples. On the (*b*) $[1\,\bar{1}\,0]$ ED pattern, some $n = 2$ extra spots are clearly visible in the $[1\,1\,\bar{1}]^*$ direction. Oriented domains exist inside the grain as shown by $n = 2$ extra spots also visible in the $[1\,1\,\bar{1}]$ direction. On the (c) $[1\,\bar{1}\,0]$ ED pattern, some $n = 3$ extra spots are clearly visible in the $[1\,1\,1]^*$ direction. Domains with different superstucture also exist inside the grain as shown by $n = 2$ extra spots visible in the same $[1\,1\,\bar{1}]$ direction. These results confirm other studies in the literature for $La_2NiO_{4.25}$ oxides [19,22,23]. Accordingly, microstructural studies show heterogeneity in $La_2NiO_{4+\delta}$ oxides for $\delta = 0.17$ and $\delta = 0.25$. This heterogeneity segregates in some domains of the crystals as it can be seen on Fig. 8. However, in order to confirm this result in all range of study, additional TEM observations are in progress to verify this assumption.

According to previous studies, the nature of the atmosphere used during the decomposition of the gel influences the phase formation and the properties of the oxides. Thus, the influence of the atmosphere has been studied on the structure and the non-stoichiometry level of the $La_2NiO_{4+\delta}$ series. This study has been done with the P1 and P2 processes.

The sols were first dehydrated and annealed in air at $T_i = 400\,^\circ$C for 12 h, with a heating rate of 100 °C/h. The grinded powders are then calcined at 900 °C for 2 h under different partial oxygen pressures, with a heating rate of 150 °C/h. Whatever the partial oxygen pressures, the XR

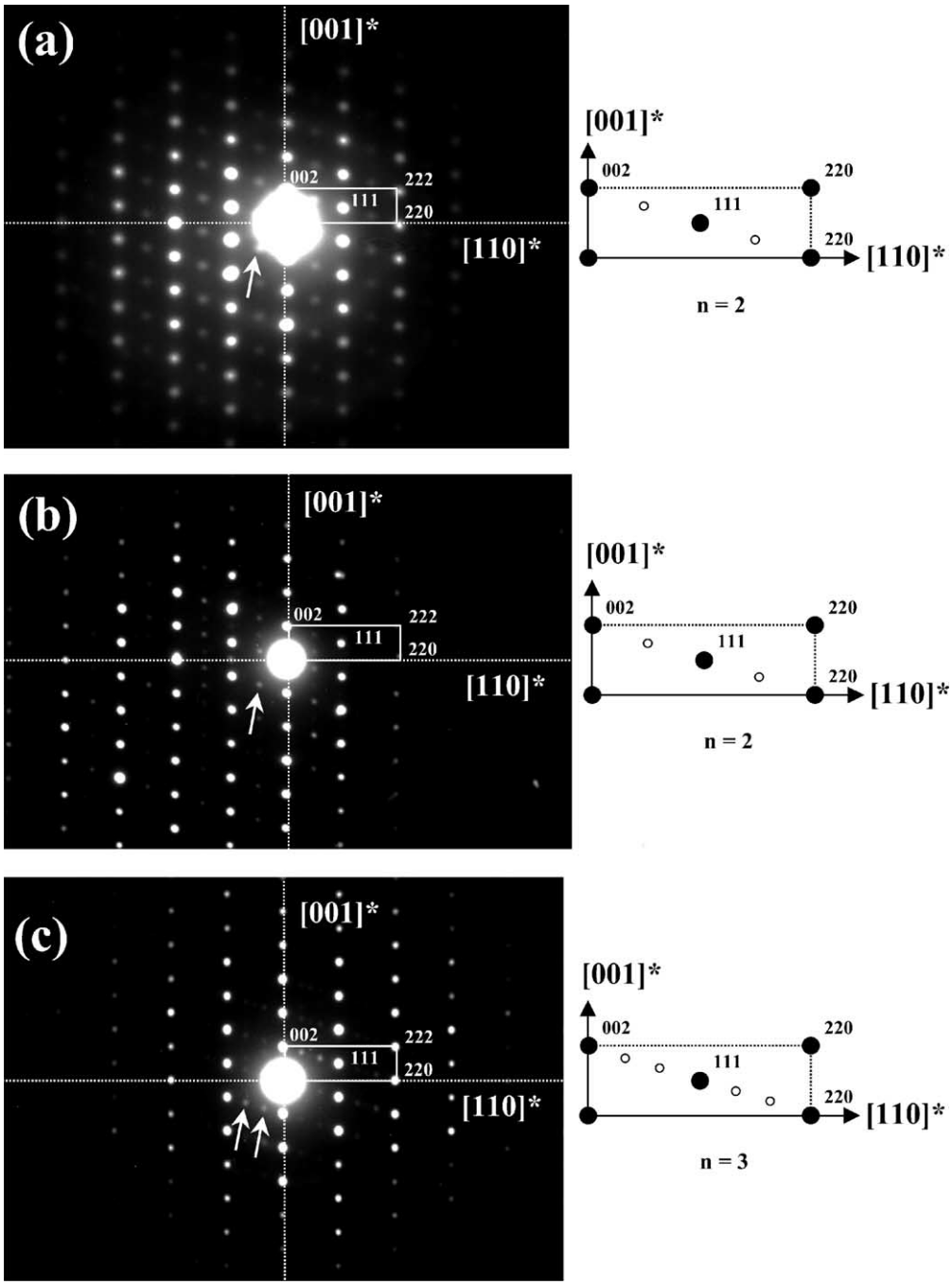

Fig. 8. [1 $\bar{1}$ 0] ED patterns for $La_2NiO_{4.19}$ (a) and for $La_2NiO_{4.25}$ (b) and (c). The $n = 2$ and $n = 3$ superlattice spots are indicated with the white arrows in the ED patterns and with open circles on the scheme.

powder diffraction patterns show impurity for both samples. This could be due to the high stabilisation of the Ni^{3+} content during the intermediate heat treatment. Previous result shows that increasing T_i does not allow the formation of the pure $La_2NiO_{4+\delta}$ phase. Thus, another intermediate heat treatment has been defined to reduce the Ni^{3+} content. After a heat treatment at $T_i = 400\,^{\circ}C$, the grinded powders are annealed in air at $T = 600\,^{\circ}C$ for 2 h, with a heating rate of 100 °C/h. Then, the powders are annealed at 900 °C for 2 h under oxygen partial pressures. In Table 6 are summarised the XRD results for both processes as function of partial oxygen pressure. For P1 process, pure $La_2NiO_{4+\delta}$ oxides are obtained for PO_2 ranging from 0.20 to 0.75 atm. However, when working under pure oxygen, a mixture of oxides is observed. For P2 process, whatever the partial oxygen pressures, a mixture of oxides forms. Thus, the second heat treatment at $T = 600\,^{\circ}C$ does not allow reducing sufficiently the Ni^{3+} content.

Table 6
Evolution of δ as a function of partial pressure of oxygen

Type of process	Partial oxygen pressure (atm)	Phases determined from XRD studies	δ ($\pm$0.01)
P1	0.20	$La_2NiO_{4+\delta}$	0.15
	0.25	$La_2NiO_{4+\delta}$	0.18
	0.50	$La_2NiO_{4+\delta}$	0.20
	0.75	$La_2NiO_{4+\delta}$	0.24
	1.00	Mixed oxides	*X*
P2	0.20	Mixed oxides	*X*
	0.25		
	0.50		
	0.75		
	1.00		

The non-stoichiometry level has been evaluated and results are reported in Table 6. For comparison, the value of δ obtained from this powder annealed with the same heat treatment at 900 °C in air is reported.

Working in oxidising atmosphere conduces to higher non-stoichiometry levels. In particular, for $pO_2 = 0.75$ atm a significant increase of $\Delta\delta = 0.08$ is obtained. A limit of the excess oxygen content is observed around $\delta = 0.25$.

This is probably due to the stabilisation of high content of Ni^{3+} cation after the intermediate heat treatment.

Finally, these results show that a limit partial oxygen pressure is required during the sol decomposition to promote the formation of the Ruddlesden–Popper phase. Then, working in air or under controlled oxygen partial pressures conduces to the formation of the $La_2NiO_{4+\delta}$ oxide with a non-stoichiometry level variable.

4. Conclusions

We synthesized $La_{2-x}NiO_{4+\delta}$ oxides ($x \geq 0$) at temperatures above 700 °C via a sol–gel route. This polymeric route allows the synthesis of Ruddlesden–Popper oxide with a controlled non-stoichiometry level (δ) with a wide range of δ. The main factor affecting the non-stoichiometry level is the oxygen partial pressure, which can be controlled by the nature of the sol and the heat treatment profile (T_i, annealed temperature, PO_2). δ varies from 0.09 to 0.25. Some values are higher than the ones generally observed in the literature and this broad range shows the adaptability and the performances of our processes. Within our experimental study, an extrapolation between the non-stoichiometry level and the mean grain sizes has been made: the higher δ, the higher $\langle d \rangle$.

XRD data refinements show that $La_{2-x}NiO_{4+\delta}$ oxides ($x \geq 0$) have an orthorhombic symmetry (*Fmmm* space group) for $x = 0$ and crystallise in a tetragonal cell (*I4/mmm* space group) for $x > 0$.

TEM observations show heterogeneity in composition on the Ruddlesden–Popper grains, while keeping the pure phase. Indeed, for a specific formulation of the $La_2NiO_{4+\delta}$ oxide, different orderings of the excess oxygen are shown and indicate that mixed compositions of excess oxygen content are present in the oxide.

For an application in SOFC devices, $La_2NiO_{4+\delta}$ oxides are interesting because of their mixed conductivity due to the incorporation of additional oxygen on the interstitial sites. In particular, the oxygen ionic diffusion is some orders of magnitude higher than in perovskite. However, recent studies on $La_2NiO_{4.16}$ oxide show that the electrical conductivity of this oxide is quite low [17]. No test has been performed for this broad range of δ. The electrical properties can be optimised by controlling δ and the best value of δ in SOFC conditions should be define to adjust both ionic and electronic conductivities. For this challenge, our process is very interesting because of its adaptability for the control of δ and its flexibility for the elaboration of thin films.

References

[1] S.C. Singhal, Solid State Ionics 152/153 (2002) 405–410.
[2] M. Dokiya, Solid State Ionics 152/153 (383) (2002) 383–392.
[3] T. Tsai, S.A. Barnett, Solid State Ionics 93 (3/4) (1997) 207–217.
[4] H. Uchida, S. Arisaka, M. Watanabe, Solid State Ionics 135 (1–4) (2000) 347–351.
[5] S.N. Ruddlesden, P. Popper, Acta Crystallogr. 11 (1958) 54.
[6] Pechini, Patent 3,330,697, 11th July 1967.
[7] E. Boehm, Ph.D Thesis, Bordeaux, 2002.
[8] M. Gaudon, C. Laberty-Robert, F. Ansart, P. Stevens, A. Rousset, Solid State Sci. 4 (2002) 125.
[9] M.L. Fontaine, C. Laberty-Robert, F. Ansart, P. Tailhades, J. Solid State Chem., in press.
[10] M. Greenblatt, Solid State Mater. Sci. 2 (1997) 173.
[11] H. Tamura, A. Hayashi, Y. Ueda, Physica C 216 (1993) 83.
[12] J.D. Jorgensen, B. Dabrowski, S. Pei, D.R. Richards, D.G. Hinks, Phys. Rev. B 40 (1989) 2187.
[13] A. Hayashi, H. Tamura, Y. Ueda, Physica C 258 (1/2) (1996) 61–71.
[14] W.J. Jang, K. Imai, M. Hasegawa, H. Takei, J. Cryst. Growth 152 (1995) 158.
[15] A. Demourgues, A. Wattiaux, J.C. Grenier, M. Pouchard, J.L. Soubeyroux, J.M. Dance, P. Hagenmuller, J. Solid State Chem. 105 (2) (1993) 458–468.
[16] S.J. Skinner, Solid State Sci. 5 (3) (2003) 419–426.
[17] N.J. Poirot, P. Odier, P. Simon, J. Alloys Comp. 262/263 (1997) 147.
[18] Z. Hiroï, T. Obata, M. Takano, Y. Bando, Phys. Rev. B 41 (1990) 11665.
[19] A. Demourgues, F. Weill, J.C. Grenier, A. Wattiaux, M. Pouchard, Physica C 192 (3/4) (1992) 425–434.
[20] A. Rabenam, P. Eckerlin, Acta Crystallogr. 11 (1958) 304.
[21] B. Willer, M. Daire, C.R. Acad. Sci. Paris, Ser. C 267 (1968) 1482.
[22] A. Wattiaux, Habilitation dissertation, Bordeaux, 1996.
[23] Z. Hiroï, M. Takano, Y. Bando, Supercond. Sci. Technol. 4 (1991) 139.
[24] K.K. Singh, P. Ganguly, J.B. Goodenough, J. Solid State Chem. 53 (1984) 254.
[25] P. Ganguly, Ph.D. Thesis, Bordeaux 1, 1984.